A Multifrequency Polarimetric SAR Processing Chain to Observe Oil Fields in the Gulf of Mexico

Maurizio Migliaccio, *Senior Member, IEEE*, Ferdinando Nunziata, *Student Member, IEEE*,
Antonio Montuori, *Student Member, IEEE*, Xiaofeng Li, *Senior Member, IEEE*, and
William G. Pichel, *Member, IEEE*

Abstract—Within the National Environmental Satellite, Data, and Information Service, National Oceanic and Atmospheric Administration, multiplatform synthetic aperture radar (SAR) imagery is being used to aid posthurricane and postaccident response efforts in the Gulf of Mexico, such as in the case of the recent Deepwater Horizon oil spill. The main areas of interest related to such disasters are the following: 1) to identify oil pipeline leaks and other oil spills at sea and 2) to detect man-made metallic targets over the sea. Within the context of disaster monitoring and response, an innovative processing chain is proposed to observe oil fields (i.e., oil spills and man-made metallic targets) using both L- and C-band full-resolution and fully polarimetric SAR data. The processing chain consists of two steps. The first one, based on the standard deviation of the phase difference between the copolarized channels, allows oil monitoring. The second one, based on the different symmetry properties that characterize man-made metallic targets and natural distributed ones, allows man-made metallic target observation. Experiments, accomplished over single-look complex L-band Advanced Land Observing Satellite (ALOS) Phased Array type L-band Synthetic Aperture Radar (PALSAR) and C-band RADARSAT-2 fully polarimetric SAR data gathered in the Gulf of Mexico and related to the Deepwater Horizon accident, show the effectiveness of the proposed approach. Furthermore, the proposed approach, being able to process both L- and C-band fully polarimetric and full-resolution SAR measurements, can take full benefit of both the ALOS PALSAR and RADARSAT-2 missions, and therefore, it allows enhancing the revisit time and coverage which are very critical issues in oil field observation.

Index Terms—Gulf of Mexico, man-made metallic target detection, oil spill detection, synthetic aperture radar (SAR).

M. Migliaccio, F. Nunziata, and A. Montuori are with the Dipartimento per le Tecnologie, Universitá degli Studi di Napoli "Parthenope," 80143 Napoli, Italy (e-mail: maurizio.migliaccio@uniparthenope.it; ferdinando.nunziata@uniparthenope.it; antonio.montuori@uniparthenope.it).

X. Li is with the I. M. Systems Group/National Environmental Satellite, Data, and Information Service, National Oceanic and Atmospheric Administration, Camp Springs, MD 20746 USA (e-mail: Xiaofeng.Li@noaa.gov).

W. G. Pichel is with the Center for Satellite Applications and Research, National Environmental Satellite, Data, and Information Service, National Oceanic and Atmospheric Administration, Camp Springs, MD 20746 USA (e-mail: William.G.Pichel@noaa.gov).

I. INTRODUCTION

THE GULF OF Mexico is one of the largest basins in the world, located south of the U.S. and north of Mexico. It serves an important role in the worldwide economy due to its oil fields that are at the core of the petrochemical industry of the U.S. In fact, there are thousands of oil and gas rigs a few miles away from the coast running from Texas to Louisiana and the state of Mississippi. A recent estimate indicates that there are approximately, in June 2010, 3445 oil and gas structures in the Gulf of Mexico, producing, in October 2010, 29% of the oil and 13% of the natural gas produced in the U.S. [1]. However, these oil rigs pose an important environmental risk in the case of disasters and accidents, such as the recent massive Deepwater Horizon oil spill, which is considered the largest offshore spill in U.S. history.

In addition to such disasters/accidents, the Gulf of Mexico is prone to hurricanes. During such events, man-made metallic infrastructures, such as oil rigs, can be wrecked or destroyed, accompanied by release of oil at sea [2]. Therefore, both oil-at-sea monitoring and man-made metallic target observation are very important issues. They represent two complex activities that cannot be solved just by means of conventional observation techniques, i.e., coast guard ships and aerial observation. Accordingly, coastal managers are continuously interested in knowing the real-time positions of all the oil rigs, particularly after the passage of hurricanes. The main reason for such an observation is to identify possible oil pipeline leaks on the sea surface and to detect changes in man-made metallic targets, thus providing firsthand information on potential oil drilling infrastructure damage. Within such a framework, synthetic aperture radar (SAR) plays a fundamental role since it allows overcoming the constraints of *in situ* techniques and ensures improved spatial/temporal coverage. SAR is an active coherent band-limited microwave high-resolution sensor that can make daytime and nighttime measurements almost independent of atmospheric conditions. However, observing oil slicks and man-made metallic targets at sea by means of SAR is not an easy task due to both technical, e.g., false alarms, speckle, etc., and technological, e.g., spatial resolution, spatial and/or temporal coverage, etc. In this paper, for the first time, a polarimetric approach that embodies both oil slick and man-made metallic target observations is proposed. In order to properly frame this paper, the relevant state of the art is hereafter briefly summarized. Since the states of the art of SAR oil slick observation and SAR man-made metallic target detection are disjoint, they are described separately.

This article has been accepted for inclusion in a future issue of this journal. Content is final as presented, with the exception of pagination.

2   IEEE TRANSACTIONS ON GEOSCIENCE AND REMOTE SENSING

SAR oil slick observation is physically possible, under low-to-moderate wind conditions ($\sim$3–12 m/s) [3], [4], because an oil slick damps the short gravity and capillary waves and reduces the friction velocity, generating a region of low backscatter area in the SAR image [3]–[7]. However, SAR oil slick detection is not an easy task since SAR images are affected by multiplicative noise, known as speckle, which hampers interpretability of such images [4]. Furthermore, there are other physical phenomena, known as look-alikes, which can generate dark areas in SAR images not related to oil slicks, such as biogenic films (e.g., slicks produced by animals and plankton), low-wind areas, areas of wind shadow near coasts, rain cells, currents, zones of upwelling, internal waves, and oceanic or atmospheric fronts [3], [4]. Tailored filtering techniques must be developed in order to minimize the number of false alarms. Within such a context, single-polarization SAR oil slick detection procedures can be generally divided into three phases: dark area detection, feature extraction, and oil slick/look-alike classification [4], [8]–[10]. Dark area detection algorithms are generally based on filtering techniques accomplished on multilook single-polarization SAR data. While dark area detection algorithms yield the area location and the segmentation of suspected polluted areas, the extraction of features (e.g., geometric, radiometric, and texture related) is necessary to perform the classification [4], [10]. On the basis of the estimated features and some *a priori* knowledge, it is possible to assign a probability that a dark area is an oil slick. Furthermore, the usefulness of additional external data is recognized to enhance the ability to distinguish between oil slicks and look-alikes, such as local wind field information (to sort out low-wind areas) and optical data to identify biogenic films [3], [4]. Following this rationale, the importance of polarimetric SAR measurements for oil slick observation purposes has been demonstrated [11]–[19].

New quad- and dual-polarization approaches have been recently developed for sea oil slick observation, under low-to-moderate wind conditions.

Among the quad-polarization approaches, a method has been developed in [11] that combines the use of a fully polarimetric constant-false-alarm-rate (CFAR) filter and the Cloude–Pottier target decomposition (TD) theorem to better assist oil slick classification. The approach first demonstrates the effectiveness of a polarimetric CFAR filter to identify dark patches related to possible oil slicks and the usefulness of polarimetric entropy (PE) in distinguishing sea surface from both oil-covered areas and weak-damping biogenic look-alikes. On similar guidelines, biogenic slicks are characterized in [12]. An electromagnetic model, based on the Mueller matrix, was exploited in [13] to characterize the scattering mechanism of the sea surface with and without oil and biogenic slicks. The model predicts a completely different scattering mechanism for a slick-free or weak-damping slick-covered sea surface and an oil-covered one. A simple and effective filtering technique has been developed and shown to be both able to observe oil slicks and distinguish them from weak-damping look-alikes. In [14] and [15], the copolarized signature has been interpreted in terms of the sea surface scattering mechanism with and without oil slicks. It was found that the pedestal, on which the copolarized signature is set, is both able to emphasize oil slicks and de-emphasize weak-damping surfactants, with respect to the surrounding sea surface. In [16] and [17], the Mueller-matrix-based filter

[13] and the polarimetric signature approach [14] have been combined together with a PE filter [11] in order to develop a physically based approach to exploit, for the first time, fully polarimetric L-band ALOS PALSAR data for oil slick detection purposes.

A dual-polarization model has been developed in [20]–[22], which, relating the phase difference between the copolarized channels (CPD) to the sea surface scattering with and without surface slicks, allows both observing oil slicks and distinguishing them from a broad class of look-alikes, i.e., those characterized by weak-damping properties. Following this rationale, a very effective and robust approach has been implemented and successfully applied on a large data set of C-band SIR-C/X-SAR data [20], [21] and, recently, extended to X-band TerraSAR-X SAR data [22].

With respect to the state of the art related to SAR observation of man-made metallic targets at sea, both image-based and physically based approaches have been developed. The electromagnetic wave scattered off man-made metallic targets at sea is physically determined by several scattering mechanisms which cause a high coherent microwave response depending on the construction material and the characteristics of the radar instrument, such as incidence angle, frequency, polarization, resolution, and speckle [23]–[25]. Accordingly, ships and oil rigs, hereinafter man-made metallic targets, appear in SAR images as bright spots over a dark marine background. Following this rationale, many image-based techniques have been developed which seek for anomalies in SAR images [24]. However, SAR observation of man-made metallic targets at sea is a nontrivial task due to speckle and natural physical processes, e.g., atmospheric fronts, internal waves, current boundaries, breaking waves, outlying rocks, shoals, sea currents, coastal effects, etc. [24], which may generate false alarms. Accordingly, man-made metallic target detection is a complex topic that can hardly be optimized with conventional single-polarization SARs. Radiometric information provided by traditional single-channel SAR is not generally sufficient to unambiguously detect man-made metallic targets over the sea surface since it does not fully characterize the scattering mechanism of such targets [26].

New polarimetric approaches have been developed for man-made metallic target observation at sea [26]–[33]. In [26], some polarimetric detection approaches are reviewed for ship detection purposes. Both physically based approaches, e.g., coherent TD (CTD) and PE, and image-based algorithms, e.g., polarimetric CFAR and polarimetric whitening filter, are accounted for. In [27], two studies have been accomplished and tested on airborne C-band polarimetric SAR data. The first study compares target-to-clutter ratios for various polarimetric channels, demonstrating that the best polarimetric channel for ship observation purposes depends on the incidence angle. HH performs better than HV for larger incidence angles. Moreover, a comparative study on the suitability of two polarimetric TD techniques, i.e., CTD and van Zyl decomposition, is also undertaken, which demonstrates that CTD performs better than the van Zyl one in terms of false alarm rate. In [28], CTD has been enhanced in order to extend its range of applicability, and the symmetric scattering characterization method is introduced to better exploit the information provided by the symmetric scattering component in the frame of coherent scattering. In

This article has been accepted for inclusion in a future issue of this journal. Content is final as presented, with the exception of pagination.

MIGLIACCIO *et al.*: POLARIMETRIC SAR PROCESSING CHAIN TO OBSERVE OIL FIELDS IN GULF OF MEXICO

3

[29], a CFAR detector is developed which, based on the polarization cross entropy, is able to account for the different polarimetric scatterings of sea surface and ships. In [30], a multipolarization study is undertaken to develop a physically based computer-time-effective filter that is able to work on full-resolution SAR data. The study witnesses that a proper combination of speckle-related parameters, when evaluated over HV-polarized SAR data, allows detecting man-made metallic targets with a very low false alarm rate.

In this study, a new polarimetric processing chain that, taking full benefit of fully polarimetric and full-resolution SAR measurements, allows observing both oil slicks and man-made metallic targets is proposed. The processing chain consists of two steps. The first one is based on the CPD model and allows observing oil slicks by processing the copolarized (HH/VV) polarimetric channels. The second step is based on an innovative model, which is first developed to observe man-made metallic targets at sea. The model, which furthers on the seminal studies undertaken in [31]–[33], allows exploiting the different symmetry properties which characterize sea surface with and without man-made metallic targets through the correlation between the cross-polarized polarimetric channels (HH/HV). As a matter of fact, the proposed processing chain, by implementing the two aforementioned approaches, is able to effectively process fully polarimetric SAR data and to produce logical true-and-false outputs where both oil slicks and man-made metallic targets are clearly distinguishable. Experiments, undertaken on fully polarimetric single-look complex (SLC) L-band ALOS PALSAR and C-band RADARSAT-2 SAR data gathered in the Gulf of Mexico and related to the Deepwater Horizon accident, show the effectiveness of the approach.

II. ELECTROMAGNETIC MODEL

In this section, the polarimetric background relevant to sea surface scattering with and without oil slicks and man-made metallic targets is described. Thus, the two polarimetric filters are detailed. A fully polarimetric SAR measures the scattering matrix $\mathbf{S}$, which relates the field scattered off the observed scene $\mathbf{E}^s$ to the incident one $\mathbf{E}^i$ according to the Jones formalism

$$\mathbf{E}^s = \frac{e^{-jkr}}{r}\mathbf{S}\mathbf{E}^i \tag{1}$$

where $\mathbf{S}$ is a 2×2 complex matrix given by

$$\mathbf{S} = \begin{pmatrix} S_{hh}e^{j\varphi_{hh}} & S_{hv}e^{j\varphi_{hv}} \\ S_{vh}e^{j\varphi_{vh}} & S_{vv}e^{j\varphi_{vv}} \end{pmatrix} \tag{2}$$

where each complex element of the scattering matrix is termed as scattering amplitude. For a given frequency and viewing geometry, $\mathbf{S}$ depends on the scattering target properties only [34].

Equation (1) represents a first-order coherent scattering model that cannot be employed to describe the polarimetric scattering due to a generic and depolarizing distributed target, since the Jones formalism is not able to account for depolarizing

phenomena. Hence, a more general formalism, based on the Stokes parameters, must be employed [35]

$$\mathbf{s}^s = \frac{1}{(kr)^2}\mathbf{M}\mathbf{s}^i \tag{3}$$

where $\mathbf{s}^{s(i)}$ is the scattered (incident) Stokes vector and $\mathbf{M}$ is the 4×4 Mueller matrix which generally consists of 16 independent parameters. Equation (3) represents a second-order incoherent scattering model which, due to the capability of the Stokes vector to describe both fully and partially polarized waves, represents the most general way to deal with polarimetric scattering [34], [35]. The scattering configuration, e.g., the symmetry and the reciprocity properties of the medium and the scattering geometry, simplifies the Mueller matrix, reducing the number of independent parameters. In the backscattering case and assuming that the reciprocity condition is satisfied, $\mathbf{M}$ consists of nine independent parameters

$$\mathbf{M} = \begin{pmatrix} M_{11} & M_{12} & M_{13} & M_{14} \\ M_{12} & M_{22} & M_{23} & M_{24} \\ M_{13} & M_{23} & M_{33} & M_{34} \\ -M_{14} & -M_{24} & -M_{34} & M_{44} \end{pmatrix} \tag{4}$$

which, according to the backscattering alignment convention, are given by

$$M_{11} = \frac{1}{2}\left\langle \left(S_{hh}^2 + 2S_{hv}^2 + S_{vv}^2\right)\right\rangle$$

$$M_{22} = \frac{1}{2}\left\langle \left(S_{hh}^2 - 2S_{hv}^2 + S_{vv}^2\right)\right\rangle$$

$$M_{33} = \left\langle \Re\left(S_{hh}S_{vv}^* + S_{hv}^2\right)\right\rangle$$

$$M_{44} = \left\langle \Re\left(S_{hh}S_{vv}^* - S_{hv}^2\right)\right\rangle$$

$$M_{12} = M_{21} = \frac{1}{2}\left\langle \left(S_{hh}^2 - S_{vv}^2\right)\right\rangle$$

$$M_{13} = M_{31} = \left\langle \Re\left(S_{hh}S_{hv}^* + S_{hv}S_{vv}^*\right)\right\rangle$$

$$M_{14} = -M_{41} = \left\langle \Im\left(S_{hh}S_{hv}^* + S_{hv}S_{vv}^*\right)\right\rangle$$

$$M_{23} = M_{32} = \left\langle \Re\left(S_{hh}S_{hv}^* - S_{hv}S_{vv}^*\right)\right\rangle$$

$$M_{24} = -M_{42} = \left\langle \Im\left(S_{hh}S_{hv}^* - S_{hv}S_{vv}^*\right)\right\rangle$$

$$M_{34} = -M_{43} = \left\langle \Im\left(S_{hh}S_{vv}^* - S_{hv}^2\right)\right\rangle. \tag{5}$$

Although the Mueller approach represents the most general way to deal with polarimetric scattering, the Mueller matrix is not easy to understand in physical terms, and therefore, it is not widely employed to describe the polarimetric scattering [36].

A. Oil Slick Observation

An electromagnetic model has been developed in [20]–[22] which gives an understanding of the CPD in terms of the sea surface scattering mechanism with and without oil slicks under

low-to-moderate wind conditions. According to (2), the CPD is given by

$$\varphi_c = \varphi_{hh} - \varphi_{vv} \tag{6}$$

where φ_{hh} and φ_{vv} are the copolarized phases. The CPD probability density function (pdf) is related to the complex correlation between the copolarized channels $\dot{\rho}$ [20]

$$\dot{\rho} = \rho e^{j\bar{\varphi}}. \tag{7}$$

For a given look number l, the width of the CPD pdf depends on ρ, and the peak of this pdf is at $\varphi_c = \bar{\varphi}$. In particular, when ρ tends to zero (total decorrelation between the copolarized channels), the pdf becomes uniformly distributed between $[-\pi, \pi)$, while for ρ approaching one (HH and VV totally correlated), the pdf tends to a Dirac delta function. For $0 < \rho < 1$, the pdf resembles a Gaussian bell with a mean value and a standard deviation σ inversely related to ρ.

According to the model presented in [20], two cases must be distinguished under low-to-moderate wind conditions: slick-free or weak-damping slick-covered sea surface and oil-covered sea surface.

When dealing with a slick-free sea surface, Bragg or tilted-Bragg scattering mechanism is in place which, being a single-reflection scattering mechanism, calls for highly correlated copolarized channels. Accordingly, a narrow CPD pdf and, therefore, a low CPD standard deviation are expected, as demonstrated in [20].

When dealing with a weak-damping slick-covered sea surface, Bragg scattering is still in place, although characterized by a lower backscattering intensity which generates the dark area in a single-polarization SAR image. Accordingly, this case is expected to be indistinguishable from the former one in terms of CPD standard deviation, as demonstrated in [20].

When dealing with an oil-covered sea surface, due to its strong damping properties, a large departure from the Bragg scattering mechanism occurs which calls for a weak correlation between the copolarized channels. Accordingly, a broader CPD pdf and, therefore, a large CPD standard deviation are expected, as demonstrated in [20].

Based on this rationale, a simple and very effective physically based filtering technique, which estimates the CPD standard deviation in dual-polarized SAR data, has been developed and tested [20]–[22]. The approach is expected to highlight both oil slicks and man-made metallic targets with respect to the background sea surface.

B. Man-Made Metallic Target Observation

For man-made metallic target observation, an electromagnetic model has been developed to both interpret reflection symmetry in physical marine terms and relate the symmetry properties of the sea surface with and without man-made metallic targets to polarimetric observable features. Reflection symmetry is accounted for since most natural targets, i.e., the sea surface, satisfy this property [37]. On the contrary, man-made metallic targets, i.e., ships and oil rigs, being complex scatters do not follow reflection symmetry.

Within such a framework, it can be proven that reflection symmetry manifests itself by nulling the correlation between like- and cross-polarized scattering amplitudes [37]. This means that the Mueller matrix (4), when reflection symmetry applies, has only eight nonzero elements

$$\mathbf{M} = \begin{pmatrix} M_{11} & M_{12} & 0 & 0 \\ M_{12} & M_{22} & 0 & 0 \\ 0 & 0 & M_{33} & M_{34} \\ 0 & 0 & -M_{34} & M_{44} \end{pmatrix}. \tag{8}$$

It must be explicitly stated that this result applies without any reference to the specific scattering mechanism (surface scattering, volume scattering, or volume–surface scattering) and without regard to how dense the medium or how rough the surface is, as long as the scattering configuration has the corresponding symmetry [37].

Following this rationale, it is now important to understand reflection symmetry in marine terms by considering two reference scenarios: sea surface with and without man-made metallic targets.

Free sea surface, being a reflection symmetry target, is expected to call for (8), and therefore, the correlation between like- and cross-polarized scattering amplitudes HV_c

$$HV_c = \left\| \left\langle \dot{S}_{hh} \dot{S}_{hv}^* \right\rangle \right\|, \tag{9}$$

is to be expected negligible. When a man-made metallic target is present over the sea surface, due to its complex shape which consists of plane, dihedral, and trihedral structures, as well as dihedral corner reflectors and thin wires, reflection symmetry is not expected to be still satisfied. Accordingly, the full Mueller matrix (4) is expected to be in place, and therefore, the like- and cross-polarized scattering amplitudes are expected to exhibit a nonnegligible correlation. This implies that a larger HV_c value is expected.

As a matter of fact, the model predicts that the different symmetry properties which characterize the two scenarios call for completely different Mueller matrices, e.g., (4) and (8), respectively, which can be easily distinguished in polarimetric SAR measurements by looking at a particular polarimetric feature, namely, HV_c. In detail, negligible HV_c values are expected in the case of a free sea surface while significantly larger HV_c values are expected when a man-made metallic target is in place.

This model suggests a simple filtering technique which, based on HV_c, is expected to be able to highlight the presence of man-made metallic targets in dual-polarized HH/HV SAR data.

III. EXPERIMENTAL RESULTS

In this section, some thought experiments are presented to demonstrate the effectiveness of the proposed approaches for both oil slick and man-made metallic target detections.

The data set consists of one SLC quad-polarization L-band Level-1.1 ALOS PALSAR scene and three SLC fine quad-polarization C-band RADARSAT-2 SAR scenes, gathered in the Gulf of Mexico, where well-known oil slicks and man-made

This article has been accepted for inclusion in a future issue of this journal. Content is final as presented, with the exception of pagination.

MIGLIACCIO *et al.*: POLARIMETRIC SAR PROCESSING CHAIN TO OBSERVE OIL FIELDS IN GULF OF MEXICO   5

TABLE I
DATA SET

Sensor	Band	Product	Date ID	UTC	Resolution (m) $Range \times Azimuth$	Scene Size (Km) $Range \times Azimuth$	Wind Speed
ALOS PALSAR	L-band	P1.1_A	2008/01/10	$04:28:49.02$	26×4.5	30×70	$4-8$ m/s
RADARSAT-2	C-band	PDS_01141700	2010/05/15	$11:56:36.993$	5.2×7.5	25×25	$4-7$ m/s
RADARSAT-2	C-band	PDS_01141710	2010/05/15	$11:56:39.295$	5.2×7.5	25×25	$4-7$ m/s
RADARSAT-2	C-band	PDS_01141720	2010/05/15	$11:56:42.596$	5.2×7.5	25×25	$4-7$ m/s

TABLE II
CPD STANDARD DEVIATION AND HV_c VALUES MEASURED WITHIN SOME THOUGHT ROIS

Product ID	Sensor	Oil CPD σ	Sea CPD σ	Ship CPD σ	Sea HV_c Correlation	Oil HV_c Correlation
P1.1_A	ALOS PALSAR	$91.8°$	$27.7°$	$54.6°$	0.007	1.201
PDS_01141700	RADARSAT-2	$50.2°$	$31.2°$	$75.5°$	0.001	0.588
PDS_01141710	RADARSAT-2	$49.5°$	$31.8°$	$81.5°$	0.003	0.448
PDS_01141720	RADARSAT-2	$50.5°$	$31.9°$	$77.8°$	0.004	0.514

metallic targets are present (see Table I). For each SAR datum, wind information has been obtained by external European Centre for Medium-Range Weather Forecasts data and by a SAR-based inversion technique [38], [39]. In all the data, the two sources of wind speeds were congruent and relevant to low-to-moderate wind conditions (see Table I).

SAR data have been processed according to the aforementioned two-step processing chain. The first step consists in applying the CPD standard deviation approach to observe oil slicks at sea. A simple and very effective physically based filtering technique has been developed which estimates CPD standard deviation in dual-polarized SLC L- and C-band SAR data by means of an $N \times N$ moving window. The second step consists in applying the reflection symmetry approach to observe man-made metallic targets. A simple physically based filtering technique has been developed which estimates (9) in fully polarimetric SLC SAR data by means of an $N \times N$ average moving window. Both filters implement a 5×5 window because it represents a good compromise between speckle smoothing and detection of small targets.

Two thought experiments are fully detailed to demonstrate the soundness of the proposed approach. Other results are summarized in Table II.

The first experiment is to process the ALOS data given in Table I, where well-known oil seepages and oil rigs are present. The HH-polarized squared modulus SAR image is shown in Fig. 1(a), where the polluted area is clearly visible while no features associated with man-made metallic targets can be easily recognized in the gray-tone image. The corresponding CPD standard deviation image is shown in Fig. 1(b), where both oil slicks and man-made metallic targets are highlighted with respect to sea surface. One can see that the CPD standard deviation values are high in areas where oil slicks and/or man-made metallic targets are present and low over the surrounding free sea surface. To provide a quantitative analysis, the CPD standard deviation values have been measured within three thought regions of interest (ROIs) relevant to sea surface (27.7°), man-made metallic targets (54.6°), and oil-covered areas (91.8°), respectively (see Fig. 1(b) and Table II). The unpredicted large

departure of the CPD standard deviation values over man-made metallic targets suggests to further the CPD approach for man-made metallic target observation purposes. However, in this study, this latter task is undertaken in the second step of the processing chain by exploiting the reflection symmetry approach whose threshold is physically set by the different symmetry properties of the targets and sea.

Here, an empirical threshold, equal to 45°, is adopted to obtain the logical true-and-false output shown in Fig. 1(c). It can be noted that both oil and man-made metallic targets have been correctly detected with respect to the background sea and coded with black and white colors, respectively.

The second step of the processing chain consists in applying the HV_c correlation filter to the cross-polarized scattering amplitudes. The HV_c filter output is shown in Fig. 2(a), where man-made metallic targets are clearly visible as white patches in the image. It can be noted that the HV_c correlation is high where man-made metallic targets are in place, while it is low both over the free sea surface and within the low backscatter area related to the oil. This suggests that reflection symmetry is everywhere in place (dark background) except within man-made metallic targets (bright patches in the image). Therefore, this result confirms that, according to the electromagnetic model described in Section II-B, man-made metallic targets are distinguished from the background marine scene by means of the HV_c correlation approach. Moreover, the experimental result confirms that symmetry properties are not strictly related to the scattering mechanism. In fact, reflection symmetry applies to both sea surface and oil slicks, which are both well distinguishable from man-made metallic targets. This is a very important result that witnesses the robustness of the proposed technique. To provide a quantitative analysis, the HV_c correlation relevant to both man-made metallic targets and sea surface has been measured within the ROIs shown in Fig. 2(a). In detail, the HV_c correlation values are 1.201 and 0.007 for man-made metallic targets and sea surface, respectively (see Table II). Since the HV_c correlation values relevant to sea surface and man-made metallic targets are well separated, a simple empirical threshold, equal to 0.02, has been

This article has been accepted for inclusion in a future issue of this journal. Content is final as presented, with the exception of pagination.

6

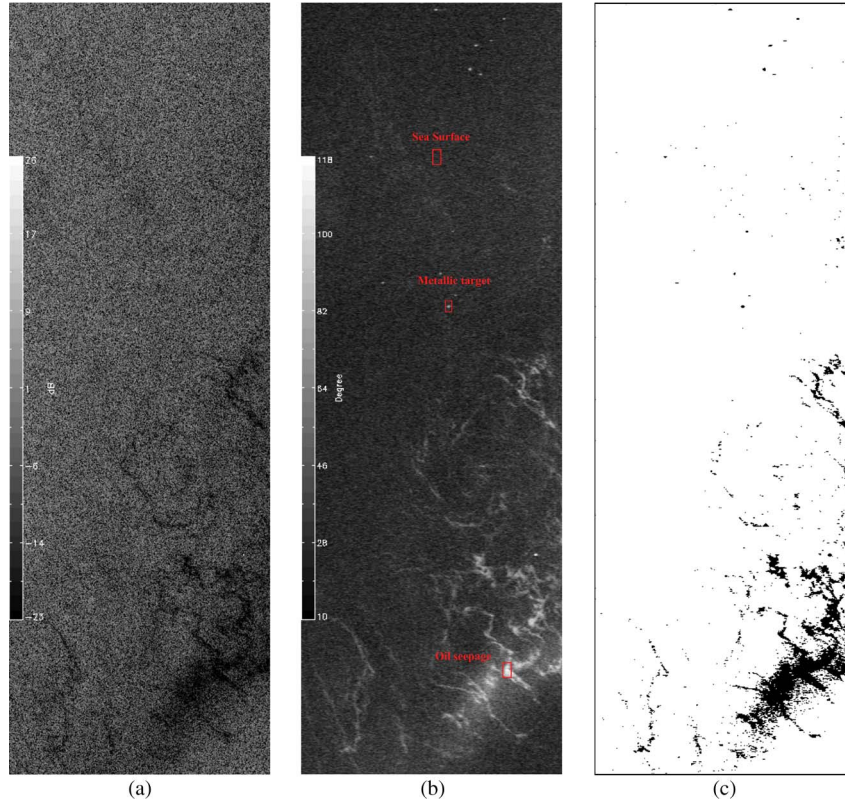IEEE TRANSACTIONS ON GEOSCIENCE AND REMOTE SENSING

Fig. 1. (a) HH-polarized squared modulus image relevant to the acquisition on January 10, 2008, site ID: ALPSRP104460550. (b) CPD standard deviation image. (c) CPD-based logical true-and-false output.
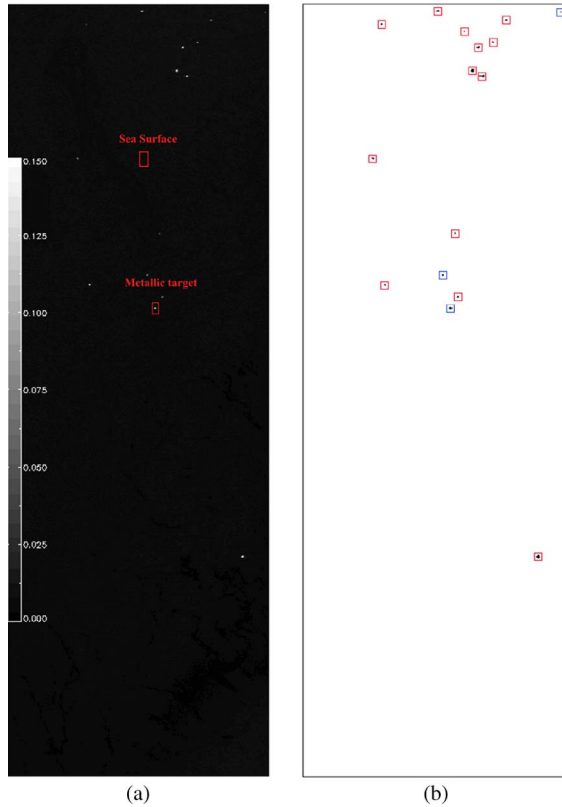

Fig. 2. (a) HV_c correlation image relevant to the acquisition on January 10, 2008, site ID: ALPSRP104460550. (b) Comparison between the HV_c-based true-and-false output and the ground truth provided in [40]. The red and blue boxes are relevant to oil rigs and ships, respectively.

applied to provide the logical true-and-false output shown in Fig. 2(b).

As a matter of fact, the second step of the proposed processing chain allows unambiguously detecting man-made metallic targets with respect to both the background sea surface and the low backscatter area. However, it must be noted that full-polarized SAR data are needed to implement the whole processing chain. A comparison between the physically based filtering results and the ground truth provided in [40] has been undertaken to classify and better distinguish different kinds of man-made metallic targets, i.e., oil platforms and ships. The obtained results are shown in Fig. 2(b), where the 13 oil rigs have been all detected and correctly located [see the red boxes in Fig. 2(b)]. Furthermore, three ships are detected in the SAR data [see the blue boxes in Fig. 2(b)]. This result shows the effectiveness of the proposed approach.

The second experiment is to process the RADARSAT-2 data in Table I. The HH-polarized squared modulus SAR image is shown in Fig. 3(a), where oil slicks, related to the Deepwater Horizon spillage, are present. Again, no features clearly associated with man-made metallic targets can be recognized in the gray-tone image. The corresponding CPD standard deviation image is shown in Fig. 3(b), where both oil slicks and man-made metallic targets are detected as bright spots over the image. The mean values of the CPD standard deviation measured over the ROIs shown in Fig. 3(b) are 50.2°, 31.2°, and 75.5° for oil, sea, and man-made metallic targets, respectively (see Table II). Even in this case, the CPD standard deviation values relevant to oil-covered sea surface are well separated from the background ones; therefore, a threshold equal to the

This article has been accepted for inclusion in a future issue of this journal. Content is final as presented, with the exception of pagination.

MIGLIACCIO *et al.*: POLARIMETRIC SAR PROCESSING CHAIN TO OBSERVE OIL FIELDS IN GULF OF MEXICO 7
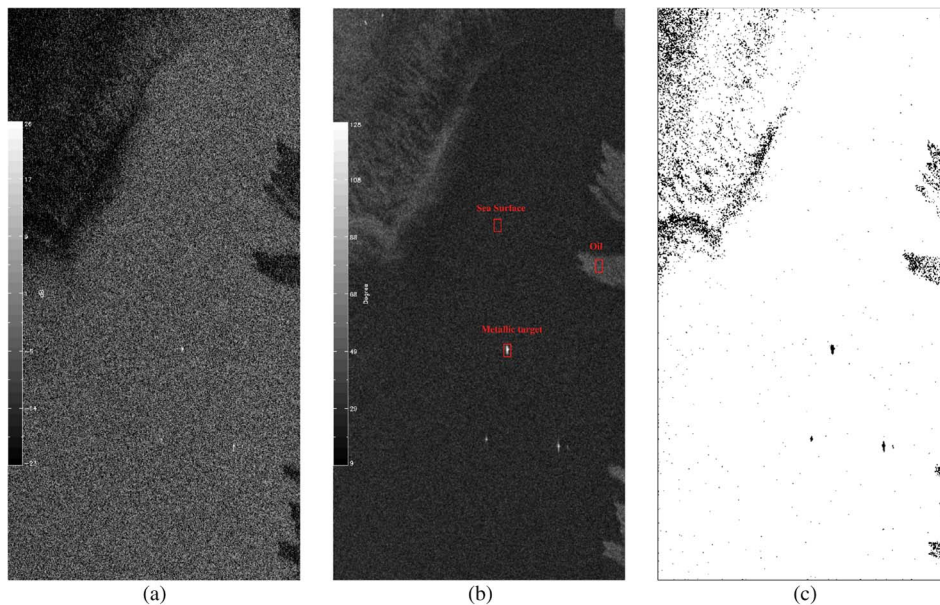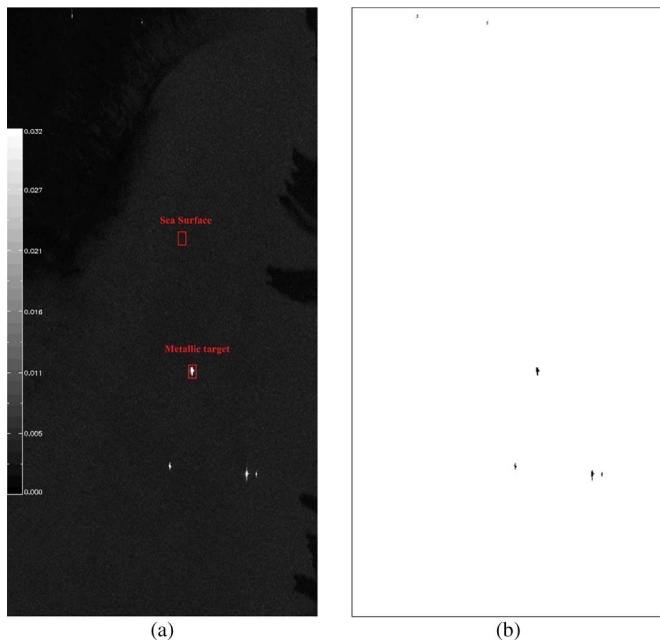

Fig. 3. (a) HH-polarized squared modulus image relevant to the acquisition on May 15, 2010 (SLC fine quad-polarization C-band RADARSAT-2 SAR data, image ID 81514, descending pass). (b) CPD standard deviation image. (c) CPD-based logical true-and-false output.

Fig. 4. (a) HV_c correlation image relevant to the acquisition on May 15, 2010 (SLC fine quad-polarization C-band RADARSAT-2 SAR data, image ID 81514, descending pass). (b) HV_c-based logical true-and-false output.

previous CPD one has been applied to provide the logical true-and-false output shown in Fig. 3(c).

To discriminate man-made metallic targets from the low backscatter area, the HV_c approach is applied to the cross-polarized scattering amplitudes, and the output is shown in Fig. 4(a). It can be noted that man-made metallic targets are clearly visible as white patches in the image, and also in this case, the proposed approach does not exhibit any sensitivity to the presence of oil slicks. The HV_c correlation values measured over the ROIs shown in Fig. 4(a) (see the red boxes in the image) are 0.588 and 0.001 for man-made metallic targets and

sea surface, respectively. Even in this case, the HV_c correlation values relevant to sea surface and man-made metallic targets are well separated. Therefore, following the same guideline of the previous experiment, a logical true-and-false output has been obtained using the same threshold (0.02) [see Fig. 4(b)].

Further experiments, undertaken on the RADARSAT-2 SLC SAR data, agree to what was formerly experienced (see Table II) and confirm the soundness of the proposed processing chain.

IV. CONCLUSION

In this paper, an electromagnetically based processing chain which makes full benefit of quad-polarization SLC SAR data has been proposed for sea oil field observation, i.e., to observe both oil slicks and man-made metallic targets. The processing chain is computer time effective (a quad-polarization SAR datum is processed in about 20 s). It is operationally oriented since it is able to both produce logical true-and-false outputs and exploit both L- and C-band polarimetric SAR data, ensuring a denser spatial/temporal coverage. As a matter of fact, the proposed processing chain is amenable to be exploited for operational purposes.

This article has been accepted for inclusion in a future issue of this journal. Content is final as presented, with the exception of pagination.

8   IEEE TRANSACTIONS ON GEOSCIENCE AND REMOTE SENSING

References

[1] U.S. Department of Energy. [Online]. Available: http://www.eia.doe.gov/special/gulf_of_mexico/index.cfm

[2] Y. Cheng, X. Li, Q. Xu, O. Garcia-Pineda, O. Andersen, and W. Pichel, "SAR observation and model tracking of an oil spill event in coastal waters," *Mar. Pollut. Bull.*, vol. 62, no. 2, pp. 350–363, Feb. 2011. doi:10.1016/j.marpolbul.2010.10.005.

[3] M. F. Fingas and C. E. Brown, "Review of oil spill remote sensing," *Spill Sci. Technol. Bull.*, vol. 4, no. 4, pp. 199–208, 1997.

[4] C. Brekke and A. H. S. Solberg, "Oil spill detection by satellite remote sensing," *Remote Sens. Environ.*, vol. 95, no. 1, pp. 1–13, Mar. 2005.

[5] F. Nunziata, P. Sobieski, and M. Migliaccio, "The two-scale BPM scattering model for sea biogenic slicks contrast," *IEEE Trans. Geosci. Remote Sens.*, vol. 47, no. 7, pp. 1949–1956, Jul. 2009.

[6] F. Nunziata, P. Sobieski, and M. Migliaccio, "A two-scale BPM contrast model," in *Proc. IGARSS*, Boston, MA, Jul. 6–11, 2008, pp. 593–596.

[7] M. Migliaccio, G. Ferrara, A. Gambardella, F. Nunziata, and A. Sorrentino, "A physically consistent speckle model for marine SLC SAR images," *IEEE J. Ocean. Eng.*, vol. 32, no. 4, pp. 839–847, Oct. 2007.

[8] O. Garcia-Pineda, B. Zimmer, M. Howard, W. G. Pichel, X. Li, and I. R. MacDonald, "Using SAR image to delineate ocean oil slicks with a texture classifying neural network algorithm (TCNNA)," *Can. J. Remote Sens.*, vol. 35, no. 5, pp. 411–421, 2009.

[9] P. Liu, C. Zhao, X. Li, M. He, and W. G. Pichel, "Identification of ocean oil spills in SAR imagery based on fuzzy logic algorithm," *Int. J. Remote Sens.*, vol. 31, no. 17, pp. 4819–4833, 2010, doi: 10.1080/01431161.2010.485147.

[10] A. Gambardella, G. Giacinto, M. Migliaccio, and A. Montali, "One-class classification for oil spill detection," *Pattern Anal. Appl.*, vol. 13, no. 3, pp. 349–366, Aug. 2010, doi: 10.1007/s10044-009-0164-z.

[11] M. Migliaccio, A. Gambardella, and M. Tranfaglia, "SAR polarimetry to observe oil spills," *IEEE Trans. Geosci. Remote Sens.*, vol. 45, no. 2, pp. 506–511, Feb. 2007.

[12] D. L. Schuler and J. S. Lee, "Mapping ocean surface features using biogenic slick-fields and SAR polarimetric decomposition techniques," *Proc. Inst. Elect. Eng.—Radar, Sonar Navigat.*, vol. 153, no. 3, pp. 260–270, Jun. 2006.

[13] F. Nunziata, A. Gambardella, and M. Migliaccio, "On the Mueller scattering matrix for SAR sea oil slick observation," *IEEE Geosci. Remote Sens. Lett.*, vol. 5, no. 4, pp. 691–695, Oct. 2008.

[14] F. Nunziata, M. Migliaccio, and A. Gambardella, "Pedestal height for oil spill observation," *IET Radar Sonar Navigat.*, vol. 5, no. 2, pp. 103–110, Feb. 2011.

[15] M. Migliaccio, F. Nunziata, and A. Gambardella, "Polarimetric signature for oil spill observation," in *Proc. US/EU-Baltic Int. Symp.*, Tallin, Estonia, May 27–29, 2008, pp. 1–5.

[16] M. Migliaccio, A. Gambardella, F. Nunziata, M. Shimada, and O. Isoguchi, "The PALSAR polarimetric mode for sea oil slick observation," *IEEE Trans. Geosci. Remote Sens.*, vol. 47, no. 12, pp. 4032–4041, Dec. 2009.

[17] M. Migliaccio, A. Gambardella, F. Nunziata, M. Shimada, and O. Isoguchi, "ALOS-PALSAR polarimetric SAR data to observe sea oil slicks," in *Proc. IGARSS*, Cape Town, South Africa, Jul. 12–17, 2009, pp. IV-669–IV-672.

[18] F. Nunziata, A. Gambardella, and M. Migliaccio, "A unified polarimetric approach for SAR sea oil slick observation," in *Proc. IGARSS Workshop*, Cape Town, South Africa, Jul. 12–17, 2009, pp. II-282–II-285.

[19] A. Gambardella, F. Nunziata, and M. Migliaccio, "A polarimetric sea surface backscattering model," in *Proc. IGARSS Workshop*, Cape Town, South Africa, Jul. 12–17, 2009, pp. I-192–I-195.

[20] M. Migliaccio, F. Nunziata, and A. Gambardella, "On the co-polarised phase difference for oil spill observation," *Int. J. Remote Sens.*, vol. 30, no. 6, pp. 1587–1602, 2009.

[21] F. Nunziata, A. Gambardella, and M. Migliaccio, "On the use of dual-polarized SAR data for oil spill observation," in *Proc. IGARSS*, Boston, MA, Jul. 6–11, 2008, pp. II-225–II-228.

[22] D. Velotto, M. Migliaccio, F. Nunziata, and S. Lehner, "Oil-slick observation using single look complex TerraSAR-X dual-polarized data," in *Proc. IGARSS*, Honolulu, HI, Jul. 25–30, 2010, pp. 3684–3687.

[23] K. Eldhuset, "An automatic ship and ship wake detection system for spaceborne SAR images in coastal regions," *IEEE Trans. Geosci. Remote Sens.*, vol. 34, no. 4, pp. 1010–1019, Jul. 1996.

[24] D. J. Crisp, *The State of-the-Art in Ship Detection in Synthetic Aperture Radar Imagery*, Defence Sci. Technol. Org., Port Wakefield, South Australia, May 2004, Res. Rep. DSTO-RR-0272. [Online]. Available: http://dspace.dsto.defence.gov.au/dspace/bitstream/1947/3354/1/DSTO-RR-0272%20PR.pdf

[25] A. Gambardella, F. Nunziata, and M. Migliaccio, "A physical full-resolution SAR ship detection filter," *IEEE Geosci. Remote Sens. Lett.*, vol. 5, no. 4, pp. 760–763, Oct. 2008.

[26] Z. Han and J. Chong, "A review of ship detection algorithms in polarimetric SAR images," in *Proc. ICSP*, Istanbul, Turkey, Dec. 15–17, 2004, pp. 2155–2158.

[27] M. Yeremy, J. W. M. Campbell, K. Mattar, and T. Potter, "Ocean surveillance with polarimetric SAR," *Can. J. Remote Sens.*, vol. 27, no. 4, pp. 328–344, 2001.

[28] R. Touzi and F. Charbonneau, "Characterization of target symmetric scattering using polarimetric SARs," *IEEE Trans. Geosci. Remote Sens.*, vol. 40, no. 11, pp. 2507–2516, Nov. 2002.

[29] J. Chen, Y. Chen, and J. Yang, "Ship detection using cross-entropy," *IEEE Geosci. Remote Sens. Lett.*, vol. 6, no. 4, pp. 723–727, Oct. 2009.

[30] G. Ferrara, M. Migliaccio, F. Nunziata, and A. Sorrentino, "GK-based observation of metallic targets at sea in full-resolution SAR data: A multipolarization study," *IEEE J. Ocean. Eng.*, vol. 36, no. 2, pp. 195–204, Apr. 2011.

[31] F. Nunziata, M. Migliaccio, and C. E. Brown, "RADARSAT-2 polarimetric data for ship observation," in *Proc. SeaSAR*, Frascati, Italy, Jan. 25–29, 2010.

[32] F. Nunziata, X. Li, M. Migliaccio, A. Montuori, and W. Pichel, "Metallic objects and oil spill detection with multi-polarization SAR," in *Proc. IGARSS*, Honolulu, HI, Jul. 25–30, 2010, pp. 2765–2768.

[33] F. Nunziata, M. Migliaccio, and C. E. Brown, "A physically-based approach to observe ships in dual-polarized SAR data," in *Proc. IGARSS*, Honolulu, HI, Jul. 25–30, 2010, pp. 3007–3010.

[34] A. Guissard, "Mueller and Kennaugh matrices in radar polarimetry," *IEEE Trans. Geosci. Remote Sens.*, vol. 32, no. 3, pp. 590–597, May 1994.

[35] J. J. van Zyl, C. H. Papas, and C. Elachi, "On the optimum polarization of incoherently reflected waves," *IEEE Trans. Antennas Propag.*, vol. AP-35, no. 7, pp. 818–825, Jul. 1987.

[36] S. R. Cloude and E. Pottier, "A review of target decomposition theorems in radar polarimetry," *IEEE Trans. Geosci. Remote Sens.*, vol. 34, no. 2, pp. 498–518, Mar. 1996.

[37] S. V. Nghiem, S. H. Yueh, R. Kwok, and F. K. Li, "Symmetry properties in polarimetric remote sensing," *Radio Sci.*, vol. 27, no. 5, pp. 693–711, 1992.

[38] E. Korsbaken, J. A. Johannessen, and O. M. Johannessen, "Coastal wind field retrievals from ERS synthetic aperture radar images," *J. Geophys. Res.*, vol. 103, no. C4, pp. 7857–7874, 1998.

[39] V. Kerbaol, B. Chapron, and P. W. Vachon, "Analysis of ERS-1/2 synthetic aperture radar wave mode imagettes," *J. Geophys. Res.*, vol. 103, no. C4, pp. 7833–7846, 1998.

[40] Minerals Management Service (MMS), *Camera Oil Platforms in the Gulf of Mexico*. [Online]. Available: http://www.gomr.mms.gov/homepg/pubinfo/repcat/arcinfo/index.html

Maurizio Migliaccio (M'91–SM'00) was born in Napoli, Italy, in 1962. He received the Laurea degree in electronic engineering from the Universitá degli Studi di Napoli "Federico II," Napoli, in 1987.

He was a Visiting Scientist at the German Aerospace Center (DLR), Oberpfaffenhofen, Germany. He is currently a Full Professor of electromagnetics with the Universitá degli Studi di Napoli "Parthenope," Napoli, where he teaches microwave remote sensing. He has also lectured in the U.S., Spain, Germany, and Italy. He has also published more than 150 papers on applied electromagnetics.

Dr. Migliaccio was the recipient of the IEEE Geoscience and Remote Sensing Society (GRS-S) Chapter Excellence Award in 2007 and the IEEE GRS-S Letters Prize Paper Award in 2009. He was also the Chapter Chair of IEEE GRS-S. He was the European Union Secretary of the COST 243 Action. He was the IEEE Italy Section Graduate of Last Decade (GOLD) delegate. He was also the General Chairman of the 2008 and 2010 IEEE GOLD Remote Sensing Conferences, both held in Frascati, Roma, at the European Space Agency and at the Italian Naval Academy in Livorno. He is a member of the Italian Space Agency (ASI) Scientific Board. He is also a member of the Scientific Board of the *Indian Journal of Radio and Space Physics*.

This article has been accepted for inclusion in a future issue of this journal. Content is final as presented, with the exception of pagination.

MIGLIACCIO *et al.*: POLARIMETRIC SAR PROCESSING CHAIN TO OBSERVE OIL FIELDS IN GULF OF MEXICO

9

Ferdinando Nunziata (S'03) was born in Italy in 1982. He received the B.Sc. and M.Sc. degrees (*summa cum laude*) in telecommunications engineering and the Ph.D. degree (curriculum electromagnetic fields) from the Universitá degli Studi di Napoli "Parthenope," Napoli, Italy, in 2003, 2005, and 2008, respectively.

Since 2010, he has been a Researcher in electromagnetic fields with the Faculty of Engineering "G. Latmiral," Universitá degli Studi di Napoli "Parthenope." He has been a Lecturer at the National Oceanography Centre, Southampton, U.K., the Université catholique de Louvain, Louvain-la-Neuve, Belgium, the Helsinki University of Technology (TKK), Espoo, Finland, and the City College of New York, New York. He is the author/coauthor of more than 70 papers published in peer-reviewed journals and refereed conferences. His main research interests include electromagnetic modeling, single- and multipolarization sea surface scattering, radar polarimetry, and synthetic aperture radar sea oil slick monitoring.

Dr. Nunziata was the recipient of the 2003 IEEE GRS South Italy Chapter Best Remote Sensing Thesis Award and the 2009 Sebetia-Ter International Award for his research activities in remote sensing. He was in the Organizing Committee of the 2008 and 2010 IEEE Graduate of Last Decade Remote Sensing Conferences at the European Space Agency and at the Italian Naval Academy in Livorno. He served as a session chair at 2008 IEEE International Geoscience and Remote Sensing Symposium, Boston, MA. He is the Chairman of the Universitá degli Studi di Napoli "Parthenope" IEEE Student Branch.

Antonio Montuori (S'09) was born in Italy in 1982. He received the B.S. and M.Sc. degrees in telecommunications engineering with full marks from the Universitá degli Studi di Napoli "Parthenope," Napoli, Italy, in 2004 and 2008, respectively, where he has been working toward the Ph.D. degree since January 2010.

In 2009, he joined the Electromagnetic and Remote Sensing Laboratory (ETA), Universitá degli Studi di Napoli "Parthenope," where he studied and developed polarimetric models for synthetic aperture radar (SAR) observation of surfactants and ships at sea. His research activity deals with single- and multipolarization electromagnetic scattering models, radar polarimetry, SAR oil and ship monitoring, and SAR-based wind estimation.

Xiaofeng Li (SM'11) received the B.S. degree in optical engineering from Zhejiang University, Hangzhou, China, in 1985, the M.S. degree in physical oceanography from The First Institute of Oceanography (FIO), State Oceanic Administration, Qingdao, China, in 1992, and the Ph.D. degree in physical oceanography from North Carolina State University, Raleigh, in 1997. During his M.S. program, he completed the course work at the Department of Physics, University of Science and Technology of China, Hefei, China.

From 1985 to 1992, he studied and worked at FIO. Since 1997, he has been with the National Environmental Satellite, Data, and Information Service (NESDIS), National Oceanic and Atmospheric Administration, Camp Springs, MD. His research interests include remote sensing observation and theoretical/numerical model studies of various types of oceanic and atmospheric phenomena, image processing, ocean surface oil spill and target detection with multipolarization synthetic aperture radar, and sea surface temperature algorithm development. He is also involved in developing many operational satellite ocean remote sensing products at NESDIS.

William G. Pichel (M'94) received the B.S. degree in physics from the University of Florida, Gainesville, in 1969 and the M.S. degree in physical oceanography from the University of Hawaii, Honolulu, in 1979.

Since 1970, he has been with the National Environmental Satellite, Data, and Information Service (NESDIS), National Oceanic and Atmospheric Administration (NOAA), Camp Springs, MD. His past assignments have included Product Area Leader for oceanographic products and Chief of the Product Systems Branch. Since 1988, he has been a Physical Scientist with the Satellite Oceanography and Climatology Division, Center for Satellite Applications and Research, NESDIS, where he is the Chair of the Sea Surface Roughness Science Team and NESDIS Point of Contact to the NOAA Marine Debris Program. His research interests include the development of ocean and hydrologic applications of synthetic aperture radar (SAR) data and the improvement of sea surface temperatures (SSTs) from satellite infrared measurements.

Mr. Pichel was a recipient of four Department of Commerce Bronze Medals for his work in SST and SAR and one Silver Medal for his work in marine debris detection at sea.